



ARL-MR-0936 • Aug 2016



# **Design of a Simple Blast Pressure Gauge Based on a Heterodyne Velocimetry Measuring Technique**

**by Michael B Zellner, Charles L Randow, Ronald Cantrell,  
Corey E Yonce, Robin Strickland, James A Perrella,  
Joshua M Sturgill, Gerald Schafer, Martin L Potter,  
Crist A Burns, Steven W Alleyne, James M Freburger,  
Seth T Halsey, Robert W Borys Sr, Kenneth W Dudeck,  
and Chester A Benjamin**

## **NOTICES**

### **Disclaimers**

The findings in this report are not to be construed as an official Department of the Army position unless so designated by other authorized documents.

Citation of manufacturer's or trade names does not constitute an official endorsement or approval of the use thereof.

Destroy this report when it is no longer needed. Do not return it to the originator.



# **Design of a Simple Blast Pressure Gauge Based on a Heterodyne Velocimetry Measuring Technique**

**by Michael B Zellner, Charles L Randow, Ronald Cantrell,  
Corey E Yonce, Robin Strickland, James A Perrella,  
Joshua M Sturgill, Gerald Schafer, Martin L Potter,  
Crist A Burns, Steven W Alleyne, James M Freburger,  
Seth T Halsey, Robert W Borys Sr, Kenneth W Dudeck,  
and Chester A Benjamin**

***Weapons and Materials Research Directorate, ARL***

REPORT DOCUMENTATION PAGE				Form Approved OMB No. 0704-0188	
<p>Public reporting burden for this collection of information is estimated to average 1 hour per response, including the time for reviewing instructions, searching existing data sources, gathering and maintaining the data needed, and completing and reviewing the collection information. Send comments regarding this burden estimate or any other aspect of this collection of information, including suggestions for reducing the burden, to Department of Defense, Washington Headquarters Services, Directorate for Information Operations and Reports (0704-0188), 1215 Jefferson Davis Highway, Suite 1204, Arlington, VA 22202-4302. Respondents should be aware that notwithstanding any other provision of law, no person shall be subject to any penalty for failing to comply with a collection of information if it does not display a currently valid OMB control number.</p> <p><b>PLEASE DO NOT RETURN YOUR FORM TO THE ABOVE ADDRESS.</b></p>					
1. REPORT DATE (DD-MM-YYYY) August 2016		2. REPORT TYPE Memorandum Report		3. DATES COVERED (From - To) 2015 October–2016 September	
4. TITLE AND SUBTITLE Design of a Simple Blast Pressure Gauge Based on a Heterodyne Velocimetry Measuring Technique				5a. CONTRACT NUMBER	
				5b. GRANT NUMBER	
				5c. PROGRAM ELEMENT NUMBER	
6. AUTHOR(S) Michael B Zellner, Charles L Randow, Ronald Cantrell, Corey E Yonce, Robin Strickland, James A Perrella, Joshua M Sturgill, Gerald Schafer, Martin L Potter, Crist A Burns, Steven W Alleyne, James M Freburger, Seth T Halsey, Robert W Borys Sr, Kenneth W Dudeck, and Chester A Benjamin				5d. PROJECT NUMBER AH80	
				5e. TASK NUMBER	
				5f. WORK UNIT NUMBER	
7. PERFORMING ORGANIZATION NAME(S) AND ADDRESS(ES) US Army Research Laboratory Weapons and Materials Research Directorate ATTN: RDRL-WMP-D Aberdeen Proving Ground, MD 21005-5069				8. PERFORMING ORGANIZATION REPORT NUMBER  ARL-MR-0936	
9. SPONSORING/MONITORING AGENCY NAME(S) AND ADDRESS(ES)				10. SPONSOR/MONITOR'S ACRONYM(S)	
				11. SPONSOR/MONITOR'S REPORT NUMBER(S)	
12. DISTRIBUTION/AVAILABILITY STATEMENT Approved for public release; distribution is unlimited.					
13. SUPPLEMENTARY NOTES					
14. ABSTRACT This report describes the construction, functionality, and optimization of a Photonic Doppler Velocimetry- (PDV-) based disposable blast pressure gauge. The gauge works on the principle that a blast wave propagating through a medium such as air, incident normal to a nondeformable disk, will accelerate the disk proportional to the difference in the pressure fields established at its incident and rear surfaces. To accurately assess these pressures, one can employ a computational method bounded by the experimentally measured acceleration of the disk within the gauge (Peng W, Zang Z, Gogos G, Gazonas G. Fluid structure interactions for blast wave mitigation. J Appl Mech. 2011;78:031016-1). The gauge was deployed in an experiment during which the blast pressure was measured from detonation of 114 g of Primasheet 1000 high explosive. The gauge reported similar results to continuum simulations using Velodyne continuum mechanics code; however, it suggests that Velodyne underpredicts the puck acceleration, and therefore the magnitude of the blast pressure front, by approximately 17%.					
15. SUBJECT TERMS blast, pressure gauge, flyer plate, overpressure, photonic Doppler velocimetry, PDV					
16. SECURITY CLASSIFICATION OF:			17. LIMITATION OF ABSTRACT  UU	18. NUMBER OF PAGES  24	19a. NAME OF RESPONSIBLE PERSON Michael B Zellner
a. REPORT Unclassified	b. ABSTRACT Unclassified	c. THIS PAGE Unclassified			19b. TELEPHONE NUMBER (Include area code) 410-278-1183

## **Contents**

---

<b>List of Figures</b>	<b>iv</b>
<b>List of Tables</b>	<b>iv</b>
<b>Acknowledgments</b>	<b>v</b>
<b>1. Introduction</b>	<b>1</b>
<b>2. Results and Discussion</b>	<b>1</b>
<b>3. Conclusions</b>	<b>12</b>
<b>4. References</b>	<b>13</b>
<b>Distribution List</b>	<b>15</b>

## List of Figures

Fig. 1	Schematic depicting blast pressure interactions with a free-flying plate.....	2
Fig. 2	Schematic (A) and photograph (B) of a blast pressure gauge that uses a heterodyne velocimetry measuring technique .....	3
Fig. 3	Depiction of a robustly mounted blast pressure gauge, with a shock isolating Neoprene layer, used to measure shock loading on an aluminum support structure .....	4
Fig. 4	Photographs of numerous techniques used to loosely hold a disk within the blast pressure gauge and the images depicting how the disk was ejected when subject to an air blast.....	6
Fig. 5	Schematic depicting the shock propagation geometry within a blast pressure gauge.....	7
Fig. 6	Photograph of the experimental setup used to validate a blast pressure gauge .....	8
Fig. 7	Multipanel image showing (A) the spectrogram resultant from the blast pressure gauge from the experiment shown in Fig. 6, (B) the extracted acceleration calculated by taking the derivative of data extracted in panel A, and (C) the computed $\Delta P$ to which the disk within the blast gauge is subjected.....	9
Fig. 8	Overlay of the experimentally measured disk acceleration and the computed (Velodyne) disk acceleration (red) and probe acceleration (blue) .....	10
Fig. 9	The pressure fields to which the disk within the blast pressure gauge was subject as computed by Velodyne .....	10

## List of Tables

Table	Description of the disk holding methods and their qualitative results...5
-------	---

## Acknowledgments

---

The authors would like to acknowledge Steven Schraml of RDRL-WMP-D and George Gazonas of RDRL-WMM-B for enlightening conversations pertaining to analysis of the gauge response.

INTENTIONALLY LEFT BLANK.



## 1. Introduction

---

Within the armor development community, there is a need to develop a compact, disposable, high-fidelity blast gauge to measure overpressures associated with harsh events, such as deflagration of energetics or detonation of high explosive where accelerated projectiles and debris may occur. Many times, overpressures generated by such events can be a nuisance to neighboring systems and environments. Knowledge of the pressure history can allow engineers to design systems to mitigate these effects. There are numerous gauges and techniques that have been developed to measure blast pressures; however, these systems are often expensive, too bulky, too complicated, or too inaccurate to use in desired implementations. For instance, current piezoelectric-based blast pressure pencil probes from PCB Piezotronics<sup>1-3</sup> provide a solution, but the gauges cost near \$2000, are constructed of 352 g of metal (plus a BNC cable connection), are greater than 300 mm in length, and only work within specified ranges of overpressures necessitating some amount of prior knowledge of the expected overpressure to be measured.

This report describes the construction and functionality of a Photonic Doppler Velocimetry- (PDV-)<sup>4,5</sup> based blast pressure gauge, which applies enhancements within the field of velocity measuring technology to improve blast measurement technology. The gauge is relatively cheap costing near \$50, is constructed of mostly soft plastics and thin-glass-based fiber optic connectors, can be scaled in size depending upon the desired measurement, and is only limited in measurement range by the yield strength of the disk material on which the gauge is based.

## 2. Results and Discussion

---

The PDV-based pressure gauge works on the principle that a blast wave propagating through a medium such as air, incident normal to a nondeformable cylindrical disk, will accelerate the disk following Newton's second law of motion. For strong overpressures, Peng et al.<sup>6</sup> identified a computational method capable of determining the blast pressure that accounts for the pressure increase generated by a shock at the disk's rear surface. This situation is pictorially described in Fig. 1. If the disk mass and shape are known and unchanging, and complications associated with release waves generated near edges of a viable disk of finite dimensions are minimized, the acceleration history of the disk is described by

$$\frac{du_d}{dt} = \frac{\Delta p_d}{\rho_d h_d} . \quad (1)$$

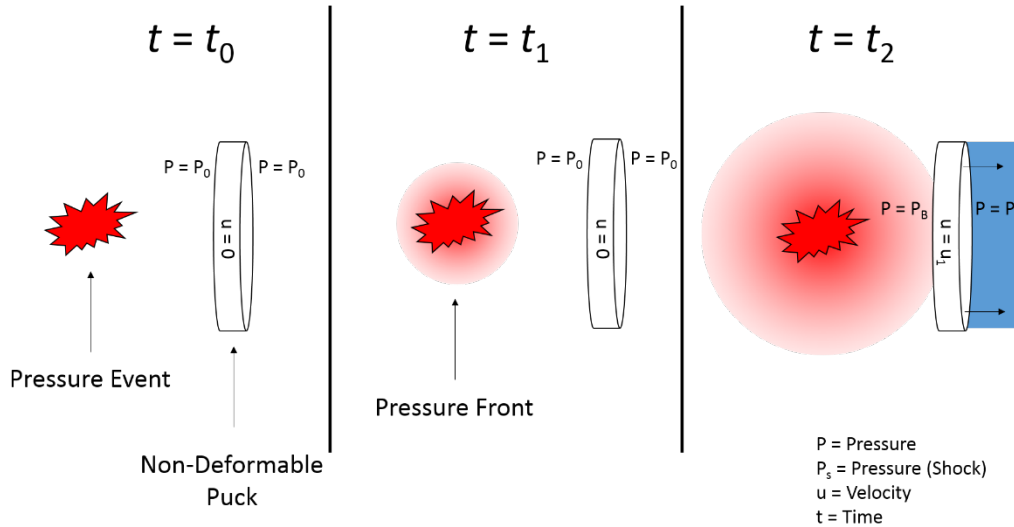


**Fig. 1 Schematic depicting blast pressure interactions with a free-flying plate**

Where  $u_d$  is the disk velocity,  $t$  is time,  $\Delta p_d$  is the difference in pressure at the front and rear surface of the disk,  $\rho_d$  is the plate density, and  $h_d$  is the plate thickness. By comparing simulations of the disk response to the experimental measurements of the disk's acceleration, one could back out the blast pressure history applied to the puck. In reality, the analysis would necessitate employment of a complete 3-dimensional geometry describing the local environment, or many simulations of finite time steps, as the blast pressure history may not follow a simplistic linear or exponential form as simplified in Peng and colleagues' computational validation.<sup>6</sup>

Figure 2 shows a schematic (A) and a photograph (B) of the device designed to make the aforementioned measurement. The device primarily consists of a metal cylinder suspended at the opening of a polymer tube using 3 skinny posts. A PDV probe is mounted at the opposite end, which is used to measure the acceleration of the disk as it is accelerated from the blast pressure. This device was constructed to accomplish the following constraints:

- The disk should not yield elastically during the event.
- The device should be capable of making an accurate position/velocity/acceleration measurement of the disk throughout the event.
- The accelerations of the disk from nonblast events should be minimized.

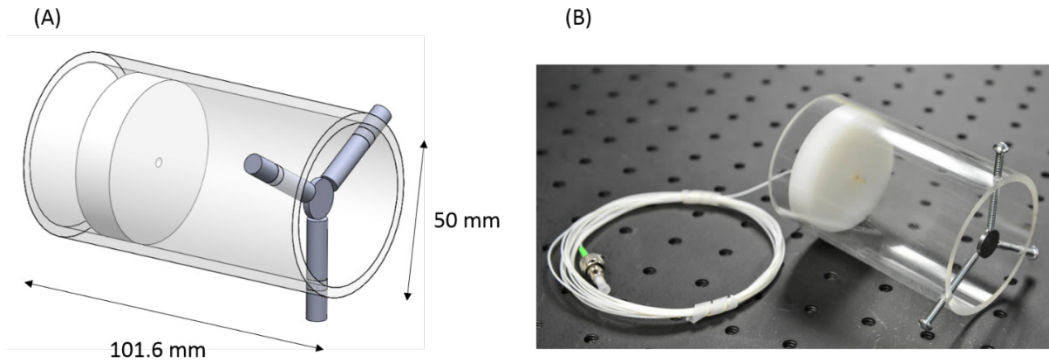


**Fig. 2 Schematic (A) and photograph (B) of a blast pressure gauge that uses a heterodyne velocimetry measuring technique**

The first constraint is dependent upon the intensity of the blast being measured. For relatively low-pressure fields, such as that generated by release of compressed air from a standard shop air compressor, the disk could be constructed using most materials such as plastics, woods, metals, and so forth. For higher intensity blasts, such as that generated by release of energy from a high-explosive detonation or deflagration, materials such as metals or ceramics may be needed. A relatively robust initial disk design applicable for blast pressures similar to that generated by detonation of high explosive of up to 10 lbs, TNT equivalent, at an offset distance of 1 m uses a cylindrical disk machined from mild steel of radius 6.4 mm, thickness 2.05 mm, and weight 2.0 g.

To address the second constraint, a single PDV channel was used to measure the acceleration history of the disk along the devices symmetry axis. This system allowed for a high-temporal profile ( $\sim 1$  ns) and high-accuracy ( $\sim 1\%$ – $2\%$ ) measurement of the disk. Because PDV is limited in its identification of the source versus target movement, it is necessary to ensure that the PDV probe is held stationary during any measurement event, or that its motion is negligible compared to the translation of the nondeformable disk when acted on by the blast front. In general, probe motion can be reduced by increasing the inertia of the probe itself. This can be accomplished via sturdy coupling of the PDV probe to the blast measuring device and attaching to a large mass via dispersive media such as a foam, neoprene rubber, or Isodamp. Figure 3 shows one example of how such a device was coupled to a large-mass metallic frame when assessing the blast loading of a Multi-Energy Flash Computed Tomography system.



**Fig. 3** Depiction of a robustly mounted blast pressure gauge, with a shock isolating Neoprene layer, used to measure shock loading on an aluminum support structure

Using a single PDV probe enables the possibility of error if the disk is rotated or translated off of the symmetry axis by a nonradially uniform pressure field. If this were the case, however, the simplistic relation to the pressure field described in Eq. 1 would be invalid and a more complicated analysis would be necessary. One could be alerted to this situation by collecting multiple co-timed PDV measurements from a few radial locations on the disk, or using a full field diagnostic (i.e., optical photography) to record the disk movement.

To address the third constraint, efforts were made to ensure that the disk was initially mounted in an axis-symmetric fashion, the disk was weakly coupled to initial external mounting, and influences that could perturb a planar or spherically symmetric blast front were minimized throughout the measurement. Of these efforts, ensuring that the disk was weakly coupled mounted in a planar, axis-symmetric fashion was found to be the most important. By design, the gauge was constructed using 3 threaded rods to “press-fit-hold” the disk in space. The threaded rods allowed for both tension adjustment of the “press-fit” and precise control to center the disk. To assess the best method of coupling the disk inside the holder, empirical observations of the disk release were made using high-speed photography for many methods of disk/threaded rod coupling when subject to an air blast generated using an air compressor and nozzle. This data is summarized in the following Table and shown in Fig. 4. The coupling methods included 1) threaded rods in as-is form (not shown), 2) threaded rods prepared with conical points to minimize contact with the disk (not shown), 3) using an off-take of Whisker Biscuit bow and arrow rest in which fiber brushes were used to initially hold the disk in place, 4) solid grooved ring, 5) adding flexible rubber caps to the ends of the rods, 6) adding springs to the ends of the threaded rods, and 7) adding spring-coupled

ball bearings to the ends of the rods to reduce the friction while sustaining a suitable coupling force prior to the release from mounting. Of these, the spring-coupled ball bearing holder appeared to have the cleanest release, although the air loading was not symmetric, causing the disk to translate and rotate in a nonaxisymmetric motion. For the particular configurations tested, 6-mm nylon or steel ball bearings were epoxied to the ends of 3-mm-outside-diameter springs constructed of 0.5-mm steel wire, which were capable of exerting a maximum of 1.16 kg of force.

**Table      Description of the disk holding methods and their qualitative results**

Method	Qualitative result (10=good, 1=poor)	Description of result
Threaded rods	3	Rigid rods were inflexible resulting in compressive loading along the rod length as the disk attempted to release. In some cases this precluded the disk from releasing.
Conical pointed rods	4	Only slightly better than non-modified threaded rods resulting from smaller surface contact with the disk.
Brushes ("Whisker Biscuit")	4	Disk had increased drag during release as it "worked" its way through the bristles.
Solid w/grooved ring	5	Clean release, but complicated by possible jetting of gas through the opening of the ring.
Rubber caps	7	Clean release.
Springs	1	Flexibility of springs resulted in inability to firmly and flatly hold the disk prior to shot.
Springs w/ball bearings	9	Very clean release. Difficult to load and keep symmetric.

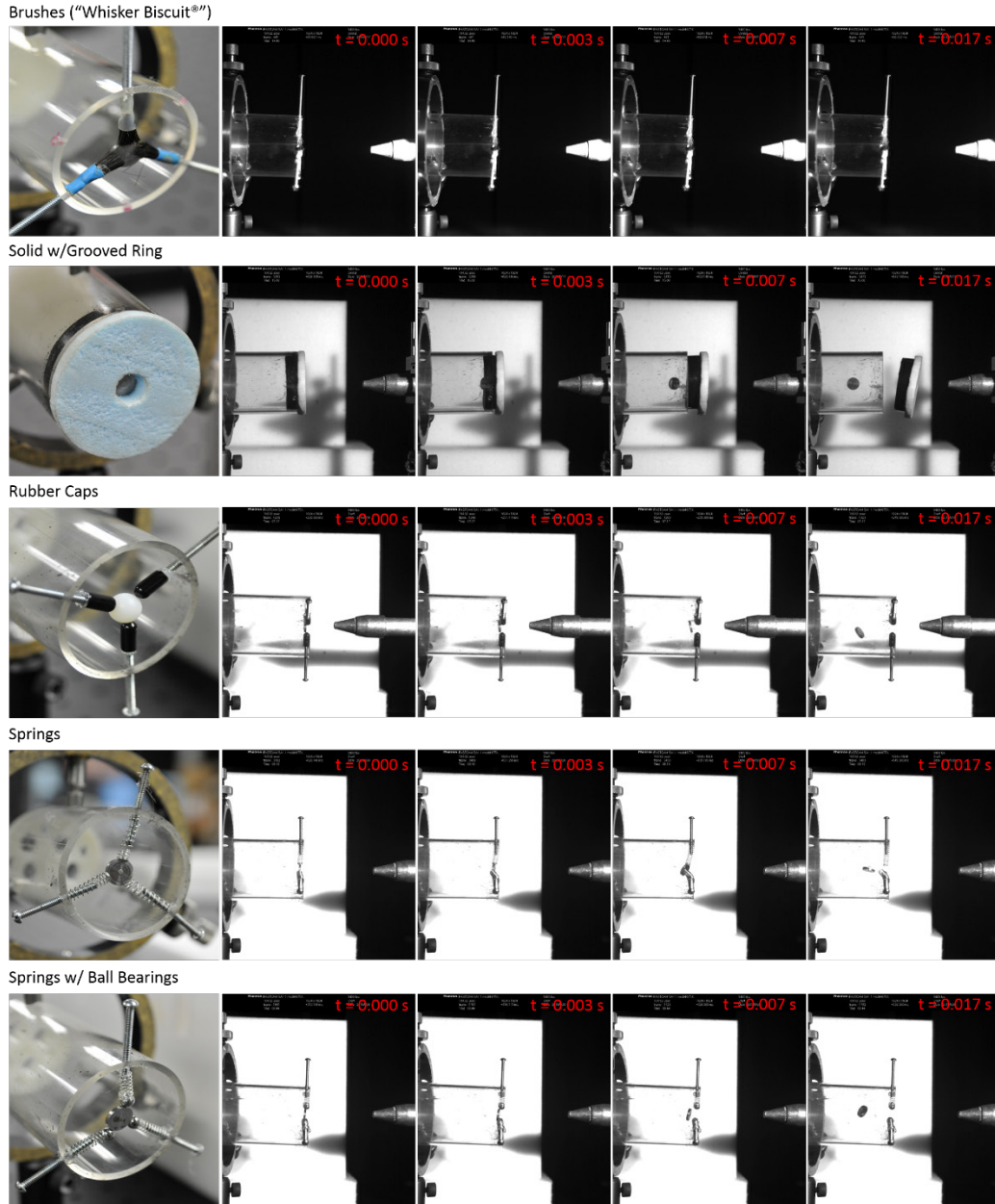


**Fig. 4 Photographs of numerous techniques used to loosely hold a disk within the blast pressure gauge and the images depicting how the disk was ejected when subject to an air blast**

To reduce device influences on the blast front and its interactions with the nondeformable disk throughout measurement, efforts were made to minimize materials interacting with the blast front in the vicinity of the disk (with the exception of the solid-grooved ring holder). In particular, the 3 threaded rods that hold the disk were symmetrically spaced and minimized in diameter. We can also delay influences of reflected waves by maximizing the boundary standoff of the diagnostic body (tube) from the disk. This is pictorially described in Fig. 5 where  $S_v$  is the wave front velocity.

Approved for public release; distribution is unlimited.



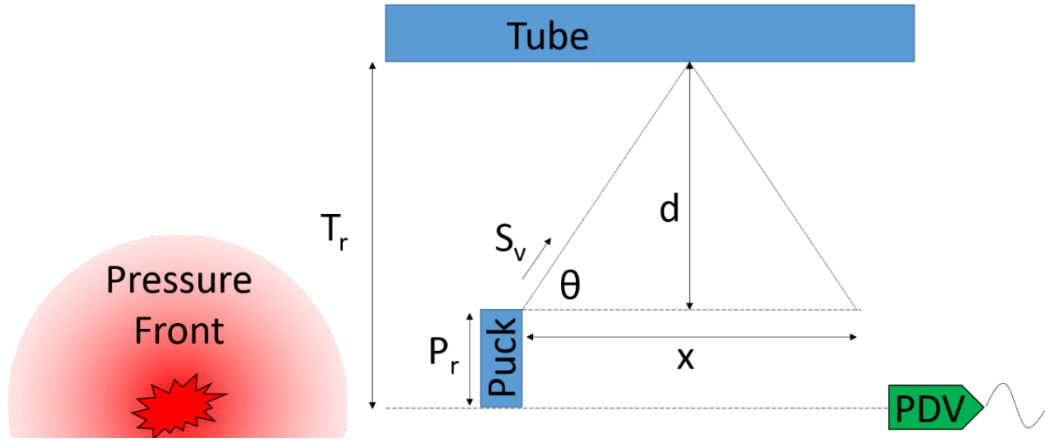


**Fig. 5** Schematic depicting the shock propagation geometry within a blast pressure gauge

The distance a reflected scattered wave must traverse ( $x_{\text{reflected}}$ ) is represented by the tightly dashed black line and

$$x_{\text{reflected}} = 2\left(\frac{d}{\sin \theta}\right) = 2\left(\frac{(T_r - P_r)}{\sin \theta}\right). \quad (2)$$

Where  $d$  and  $\theta$  are defined in Fig.5,  $T_r$  is the tube radius and  $P_r$  is the disk radius. The distance the disk travels ( $x_d$ ) in this time is proportional to the integral of the integral of the force applied by the blast front ( $F$ ) divided by the mass of the disk ( $m$ ):

$$x_d \propto \int_{t_0}^t V(u) du, \quad (3)$$

$$V(u) \propto \int_{t_0}^t \frac{F}{m} du. \quad (4)$$

Although we cannot solve these equations without additional information about the specific impulse and materials involved, we do observe that  $T_r - P_r$  is in the numerator of Eq. 2 and the disk mass is in the denominator of Eq. 4. Therefore, if we either increase the ratio of tube radius to the disk radius, or decrease the disk mass, the distance over which a pure measurement can be made will be extended.

To assess the validity of the PDV-based pressure gauge design, an experiment was performed in which 114 g of Primasheet 1000 was detonated adjacent to a gauge that used the spring/ball-bearing coupling method. The gauge was positioned 0.8 m from the center of the blast as shown in Fig. 6. The high-explosive charge was constructed of multiple sheets stacked to make an almost rectangular geometry, and was detonated from the top using a Teledyne RP-80 explosive bridge wire detonator.<sup>7</sup> From bottom to top the high-explosive stack included 5 pieces of Primasheet 1000 C-5 50 mm × 50 mm, 3 pieces of Primasheet 1000 C-1 50 mm ×

50 mm, and one piece of Primasheet 1000 C-1 25 mm × 50 mm. The total stack thickness of the 50 mm × 50 mm sheets measured to 29.7 mm, and the total thickness including all high explosive measured 30.5 mm.

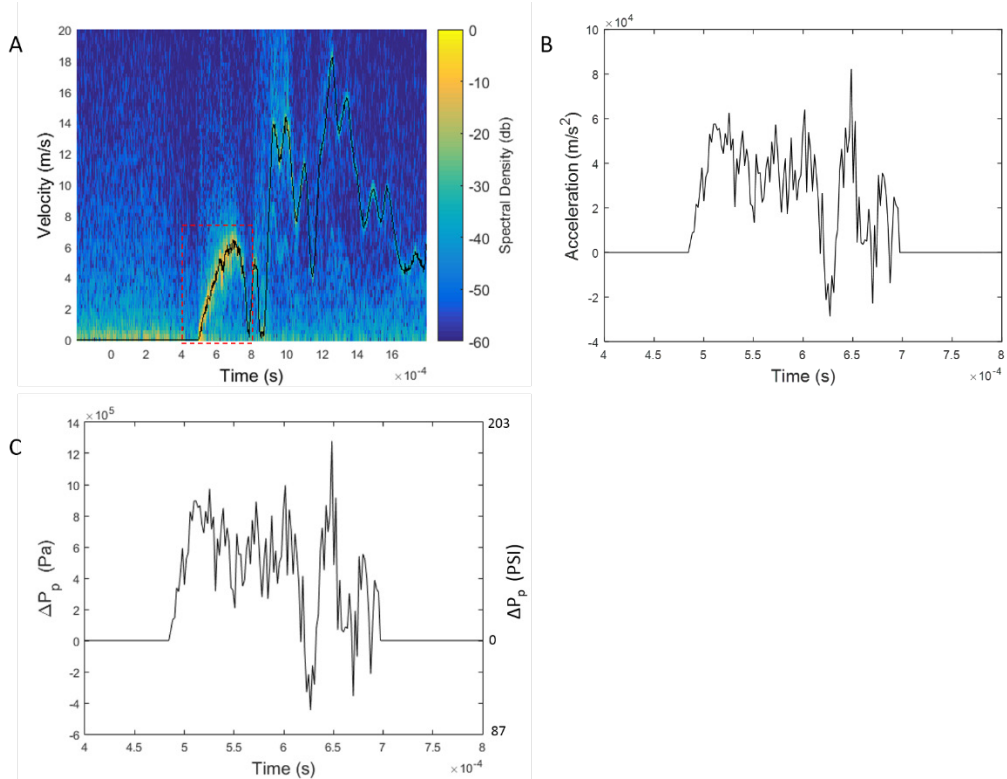


**Fig. 6 Photograph of the experimental setup used to validate a blast pressure gauge**

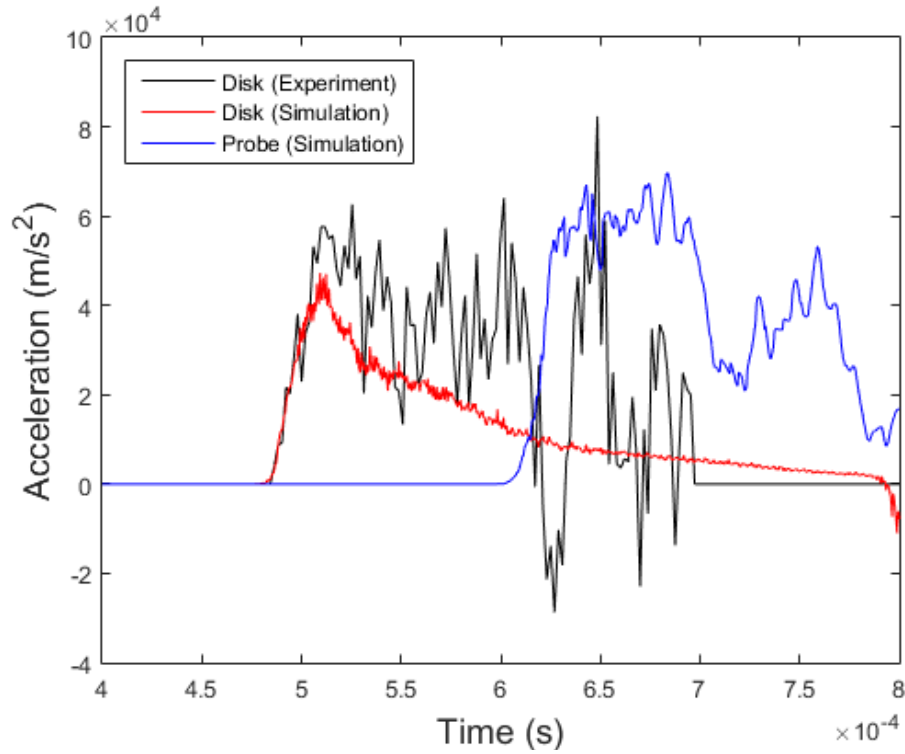
The PDV signal derived from Doppler-shifted light reflected off of the rear surface of the disk was acquired using a Third Millennium Engineering<sup>8</sup> F177a mod block coupled with a 16-GHz Keysight<sup>9</sup> digitizer bandwidth limited to 1.25 GHz. The signal was analyzed using MATLAB-based Sandia InfraRed HETrodyne aNalysis (SIRHEN) software package,<sup>10</sup> which uses a Fourier-based frequency analysis method. This combination of system and analysis provided capability to measure up to approximately 1 km/s with a temporal resolution of  $2 \times 10^{-6}$  s.

Figure 7 shows a multipanel figure including (A) the PDV spectrogram, (B) the pertinent region of disk acceleration, and (C) calculation of the difference in pressure fields applied to the disk. Figure 8 overlays the acceleration of the disk as measured with that simulated using Velodyne.<sup>11</sup> Figure 9 displays extracted pressure fields from tracers imbedded within the simulations 5 mm in front of the disk, at the disk surface, and 10 mm behind the disk surface. For the remainder of the analysis, we focus on the movement of the disk in the region outlined by the red dashed box overlaid on Fig. 7A. During this portion of the measurement, the disk translated approximately 1 mm from its initial position.





**Fig. 7** Multipanel image showing (A) the spectrogram resultant from the blast pressure gauge from the experiment shown in Fig. 6, (B) the extracted acceleration calculated by taking the derivative of data extracted in panel A, and (C) the computed  $\Delta P$  to which the disk within the blast gauge is subjected



**Fig. 8** Overlay of the experimentally measured disk acceleration and the computed (Velodyne) disk acceleration (red) and probe acceleration (blue)

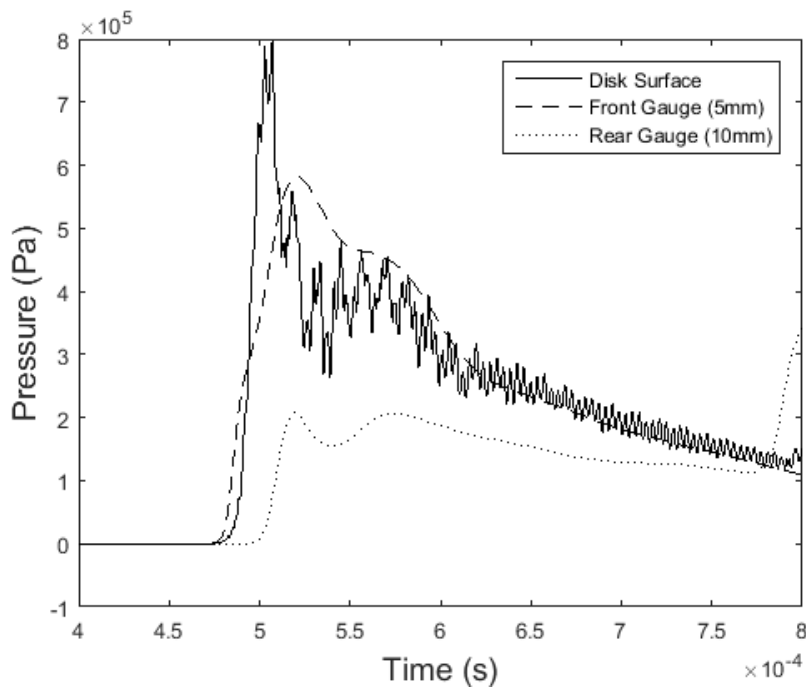


**Fig. 9** The pressure fields to which the disk within the blast pressure gauge was subject as computed by Velodyne

Experimentally, the disk begins accelerating approximately 490  $\mu\text{s}$  after detonation of the high explosive, which computes to a linear approximation of the shock velocity traveling through air at 1.63 km/s. This is significantly greater than the elastic compression velocity in air at standard temperature and pressure (0.343 km/s). The disk reaches a peak velocity of 6.36 m/s approximately 200  $\mu\text{s}$  after its initial acceleration. During this period, it was found to undergo accelerations up to 57000  $\text{m/s}^2$  (5800  $\text{g's}$ ), which corresponds with a difference in pressure near  $9 \times 10^5$  Pa (130 PSI). It is worth noting that accelerations of this magnitude are well resolved by the capabilities of the PDV system.

Comparisons of the simulations with the experimental data demonstrate similar features within the disk acceleration traces: a smooth acceleration uptake of matching slope, general overall shape to include slight general deceleration (presumably from drag and turbulence associated with the flow of high-explosive gases in air and reflection of expanding gasses off of the gauge wall surfaces), and similar temporal duration of features. The simulations reveal that the gauge geometry allows the pressure front to interact with the rear mount that holds the PDV probe approximately 120  $\mu\text{s}$  after the disk initially moves (blue trace in Fig. 8). Because PDV was fielded in the conventional manner,<sup>4</sup> one is not able to discern experimentally if velocity changes in the spectrogram are a result of the reflector accelerations or the probe accelerations. From this analysis, one can infer that the large deceleration recorded in the experimental data near 610  $\mu\text{s}$  is a result of the probe being influenced by the pressure front.

The absolute magnitude of the simulated disk acceleration peaks at 83% of that measured with the PDV blast gauge. The PDV technique is known to be capable of measuring a reflector's velocity within 1%–2% of its absolute value, indicating that simulation shortages likely account for the remaining 15% error. Because the disk acceleration has a linear dependence on the difference in pressure fields as described in Eq. 1, one can infer that the pressure fields are underestimated by approximately 15%. This discrepancy may be due to the approach used in Velodyne to model fluids and fluid structure interaction. For example, using a peak acceleration of 35000  $\text{m/s}^2$ , one would expect a corresponding pressure of 550 kPa. However, the same simulation predicts a maximum peak pressure of 350 kPa. This suggests an issue with how the pressure influences the motion of a small, relatively thin solid body.

Applying the aforementioned factors to the pressure field simulations displayed in Fig. 9 suggest that the pressure field generated by the experimental geometry peaks in the range of 8–9.2  $\times 10^5$  Pa upon interaction with the disk surface. This value is only sustained momentarily as the pressure field is increased by a factor of 2 from

reflection at the surface, but dissipates quickly back to a lower value near  $6\text{--}6.9 \times 10^5$  Pa as rarefactions propagate. These values compare well with the experimentally assessed  $9 \times 10^5$  Pa, as the shock generated behind the disk surface in this geometry is expected to be small.

### **3. Conclusions**

---

A PDV-based blast gauge was designed that provides a cost-effective, high-resolution solution toward measuring overpressures generated during blast events where accelerated ejecta and debris may be an issue. The gauge benefits from recent enhancements in measuring free surface velocities using heterodyne PDV-based techniques. The gauge design allows for low impact on experiments, applicability to a wide range of pressures, scalability in size, and is disposable.

Within the gauge design, optimization was performed to find the most suitable coupling method to hold the disk in place prior to interaction with an overpressure wave. It was found that a spring/ball-bearing coupling method produced the cleanest release of the disk with the least amount of induced rotation.

The gauge using the spring/ball-bearing coupling method was fielded in a high-explosive detonation experiment, demonstrating the ability of the gauge to measure blast overpressure. In comparisons to simulations, the response mechanics of the gauge compared well; however the simulations under predicted the accelerations (and pressure) by approximately 15%. These values may be improved if codes such as ALEGRA<sup>12</sup> or ALE3D<sup>13</sup> were used to simulate the event.

## 4. References

---

1. Walter PL. Air-blast and the science of dynamic pressure measurements. Depew (NY): PCB Piezotronics; Fort Worth (TX): Texas Christian University; 2004 [accessed 2016 July 20] <http://www.pcb.com/products.aspx?m=137B23B>.
2. MacPherson WN, Gander MJ, Barton JS, Jones JDC, Owen CL, Watson AJ, Allen RM. Blast-pressure measurement with a high-bandwidth fiber optic pressure sensor. *Meas Sci Technol*. 2000;11:95–102.
3. Manweiler RW, Chester CV, Kearny CH. Measurement of shock overpressure in air by a yielding foil membrane blast gauge. Oak Ridge (TN): Oak Ridge National Laboratory (US); 1973 Sep. Report No.: ORNL-U868.
4. Strand OT, Goosman DR, Martinez C, Whitworth TL, Kuhlrow WW. Compact system for high-speed velocimetry using heterodyne techniques. *Rev. Sci. Instr.* 2006;77:083108.
5. Doppler CJ. Über das farbige Licht der Doppelsterne und einiger anderer Gestirne des Himmels. *Abhandlungen der Koniglich Bohmischen Gessellschaft der Wissenschaften*. 1842;1:465–482.
6. Peng W, Zang Z, Gogos G, Gazonas G. Fluid structure interactions for blast wave mitigation. *J Appl Mech*. 2011;78:031016-1.
7. Teledyne RISI. Tracy (CA) [accessed 2016 July 20] <http://www.teledynenerisi.com/>.
8. TME Third Millennium Engineering [accessed 2016 July 20] <http://tmeplano.com/>.
9. Keysight Technologies [accessed 2016 July 20] <http://www.keysight.com/main/home.jsp?cc=DE&lc=ger>.
10. T Ao, Dolan DH. SIRHEN: a data reduction program for photonic Doppler velocimetry measurements. Albuquerque (NM) and Livermore (CA): Sandia National Laboratories (US); 2010 June. Sandia Report No.: SAND2010-3628.
11. Corvid Technologies, Inc. Velodyne user's manual Ver. 2.303. Mooresville (NC): Corvid Technologies, Inc.; 2013 Apr.

- 12 Robinson AC, Brunner TA, Carroll S, Drake R, Garasi CJ, Gardiner T, Haill T, Hanshaw H, Hensinger D, Labreche D, et al. ALEGRA: An arbitrary Lagrangian-Eulerian multimaterial, multiphysics code. 46th AIAA Aerospace Sciences Meeting and Exhibit; 2008 Jan 7–10; Reno (NV). AIAA 2008-1235.
13. Lawrence Livermore National Laboratory, Weapons and Complex Integration. Arbitrary Lagrangian-Eulerian 3-D and 2-D Multi-Physics Code [accessed 2016 July 20] <https://wci.llnl.gov/simulation/computer-codes/ale3d>.

1 DEFENSE TECHNICAL  
(PDF) INFORMATION CTR  
DTIC OCA

2 DIRECTOR  
(PDF) US ARMY RESEARCH LAB  
RDRL CIO L  
IMAL HRA MAIL & RECORDS  
MGMT

1 GOVT PRINTG OFC  
(PDF) A MALHOTRA

14 DIR USARL  
(PDF) RDRL WMP A  
W UHLIG  
RDRL WMP C  
B LEAVY  
RDRL WMP D  
J RUNYEON  
D PETTY  
M ZELLNER  
G VUNNI  
R DONEY  
K STOFFEL  
M KEELE  
D KLEPONIS  
A BARD  
RDRL WMP E  
D GALLARDY  
D SCHALL  
D HACKBARTH

INTENTIONALLY LEFT BLANK.